European Polymer Journal 163 (2022) 110939

Contents lists available at ScienceDirect

European Polymer Journal

journal homepage: www.elsevier.com/locate/europolj

Lytic polysaccharide monooxygenases and cellulases on the production of bacterial cellulose nanocrystals

Carolina Buruaga-Ramiro [a,b], Noelia Fernández-Gándara [a], L. Verónica Cabañas-Romero [a,b], Susana V. Valenzuela [a,b], F.I. Javier Pastor [a,b], Pilar Diaz [a,b], Josefina Martinez [a,b,*]

[a] Department of Genetics, Microbiology and Statistics, Faculty of Biology, University of Barcelona, Av. Diagonal 643, 08028 Barcelona, Spain
[b] Institute of Nanoscience and Nanotechnology (IN2UB), Universitat de Barcelona, Spain

ARTICLE INFO

Keywords:
Bacterial cellulose
Bacterial cellulose nanocrystals
Nanocomposites, cellulose enzymatic hydrolysis
Lytic polysaccharide monooxygenases

ABSTRACT

Cellulose nanocrystals are a renewable biomaterial with nanoscale properties which have useful applications. In this study, an enzymatic treatment, an approach much more environmentally friendly than the traditional harsh acid hydrolysis, was performed to obtain bacterial cellulose nanocrystals (BCNC). The combination of an oxidation by a lytic polysaccharide monooxygenase (LPMO) and a hydrolysis with a mixture of glycosyl hydrolases was effective to produce nanocrystals from bacterial cellulose. Morphology and size were confirmed by electron microscopy and laser diffraction, respectively. Thermal stability was also measured and determined to be higher relative to native bacterial cellulose. Additionally, it was found that the negative charges generated by the LPMO increased the dispersion of the nanocrystals in aqueous solution, measured by the zeta potential. The BCNC were used to coat pre-existing cellulosic materials. The obtained composites displayed improved mechanical properties, an elevated water retention capacity, and impermeability to oil. These attractive features could lead BCNC-containing polymer nanocomposites to make an impact in the field of biocompatible and biodegradable packaging materials.

1. Introduction

There is a need to create a sustainable material that could replace traditional plastic packaging. In order to reduce packaging waste created by non-degradable petroleum based packaging materials, in the last decades, there has been a rising effort to produce various biodegradable polymers for the development of edible films [1]. However, these biopolymer edible films have some limitations regarding their mechanical properties and water sensitivity. An alternative to overcome them is the use of nanomaterials, which can reinforce biopolymers by the formation of nanocomposites [2]. Nanocomposites are defined as the combination of two types of individual materials: the matrix and the material imbedded on it, being at least one of the two of nanometre-sized dimension [3]. The reinforcement provided by the nanomaterial provides improved mechanical, thermal, optical, and physicochemical properties in comparison to the polymer alone [2,4], even at very low fractions [5]. Thus, the nanometric size and the increased surface area of the reinforcing material provides this new nanocomposite unique properties [6].

From the wide range of natural resources, cellulose is the most abundant macromolecule on Earth, and it is seen as an exciting alternative to fossil-fuel plastics. In fact, cellulose nanocrystals (CNC) obtained from plant sources are commonly used as nanomaterials [7]. These CNC are highly crystalline and exhibit excellent properties like high tensile strength [8]. The conversion of cellulose fibres into nanocrystals results in the formation of the well-known whiskers, rod-like or ribbon-like shape with large aspect ratio, mainly due to their nanoscale dimensions. When compared to cellulose fibres, CNC possess many advantages apart from their appealing intrinsic nanoscale dimension such as high surface area, unique morphology, low density, renewability, biodegradability and high mechanical strength [9-11]. According to their structure, CNC have an abundance of hydroxyl groups on the active surface, which allows both, the hydrogen bonding with the fibres [12] and further functionalization [13]. The applications of CNC can be of

* Corresponding author at: Department of Genetics, Microbiology and Statistics, Faculty of Biology, Universitat de Barcelona, Av. Diagonal 643, 08028 Barcelona, Spain.
E-mail addresses: buruaga.cbr@ub.edu (C. Buruaga-Ramiro), noeliafdzgandara@gmail.com (N. Fernández-Gándara), veronica.cabanas@ub.edu (L.V. Cabañas-Romero), susanavalenzuela@ub.edu (S.V. Valenzuela), fpastor@ub.edu (F.I.J. Pastor), pdiaz@ub.edu (P. Diaz), jmartinez@ub.edu (J. Martinez).

https://doi.org/10.1016/j.eurpolymj.2021.110939
Received 23 September 2021; Received in revised form 30 November 2021; Accepted 7 December 2021
Available online 10 December 2021

two types. On the one hand, they suppose a suitable material for a wide range of applications such as synthesis of antimicrobial materials, enzyme immobilization, green catalysis, biosensing and drug delivery [14-16]. On the other hand, CNC can act as a reinforcing agent [5], with potential uses ranging from barrier films to pH sensors [17-20]. Nevertheless, bacterial cellulose (BC) is more preferred over plant cellulose for CNC obtention as it is available in relatively pure form and has better physic-chemical properties than plant cellulose [21]. BC is produced mainly by bacteria from the genera *Komagataeibacter* as an exopolysaccharide. Even though in terms of chemical structure BC is identical to the vegetal one, it is synthetized chemically pure as it does not present hemicelluloses or lignin [22]. Consequently, it does not need to be purified, reducing the economic and the environmental impact. In addition, BC displays a higher degree of crystallinity, a higher tensile strength, a higher water-holding capacity and a finer three-dimensional nanofibre network [23,24]. BC is a versatile biomaterial with numerous biotechnological applications [25]. Besides, its addition to other celluloses is well known to decrease porosity, improving barrier properties, which is interesting in packaging applications [26]. Nanocrystals derived from bacterial cellulose (BCNC) can be physically incorporated into various polymer matrices to form polymer nanocomposites [27].

CNC suspensions can be obtained by submitting native cellulose to a harsh sulfuric acid hydrolysis, often followed by ultrasound treatments, as Rånby et al. described [28]. Under this acid treatment, the amorphous regions that interconnect the crystalline regions are removed and finally, the rod-like cellulose nanocrystals are isolated [29,30]. Even if the acid hydrolysis has been improved in terms of time of hydrolysis, choice of acid and its concentration, the principle of existing technologies for conversion of cellulosic biomass into CNC has barely changed until the date. It should be noted that this method requires many hazardous chemicals, which give alarming negative impacts to the environment. Furthermore, it can affect the final properties of the CNC, compromising their potential applications [31]. Thus, it is necessary to search for new processes to produce high quality CNC, with low environmental impact and without compromising their technological or health applications. In this direction, enzymatic hydrolysis offers the potential for higher selectivity, lower energy costs and milder operating conditions than chemical processes [32]. For instance, the inclusion of an enzymatic pretreatment in the process of preparation of microfibrillated cellulose is a feasible approach, at least from kraft pulp, as Lopez-Rubio et al. [33] and Svagan et al. [34] confirmed. In the enzymatic hydrolysis of cellulose, the main involved enzymes are the cellobiohydrolases (CBH) or cellulases. To digest efficiently crystalline cellulose at least three types of CBH are known to cooperate: (1) endoglucanases (EC 3.2.1.4) that cut cellulose chains in random locations; (2) exoglucanases (EC 3.2.1.91) which peel cellulose in a processive manner on the reducing or non-reducing ends of cellulose polysaccharide chains and (3) beta - glucosidases (bGLs) (EC 3.2.2.21) which hydrolyse cellobiose and various soluble cellodextrins into glucose [31,35]. Synergistic phenomena are widely observed in cellulose hydrolysis, with many forms reported and proposed [32,36,37]. However, the accessibility of the cellobiohydrolases to the crystalline regions was difficult to understand, and authors hypothesized for decades about a “a non-hydrolytic component” that, in nature, could disrupt the cellulosic substrate, increasing its accessibility for the hydrolytic enzymes [38]. It was not until 2010 that the oxidative cleavage of cellulose glycosidic bonds was described, performed by a new type of enzyme, the lytic polysaccharide monooxygenases (LPMO) [39]. LPMOs cleave cellulose leading to the formation of aldonic acids when the C1 is oxidized and/or 4-ketoaldoses at the C4 position [40]. Since then, they have extensively been reported to promote the efficiency of cellulases during cellulose digestion [39,41,42]. They are thought to act in first place, making crystalline cellulose accessible to glycosyl hydrolases [43,44].

In this study BCNC were obtained by an environmentally friendly technique based on an exclusively enzymatic treatment of native BC. First, BC paste was treated with the enzyme SamLPMO10C, a LPMO identified and cloned in the research group [44]. Then, it was digested with a commercially available preparation of cellobiohydrolases. The obtained BCNC were characterized in terms of morphology and chemical structure by electron microscopy and X-ray diffraction, respectively, and their dispersive and thermal properties measured. Finally, BCNC were used as reinforcing agent onto pre-existing eucalyptus sheets, and the mechanical and barrier properties of the obtained composites were evaluated.

2. Methods

2.1. BC synthesis and preparation of BC

Komagataeibacter intermedius JF2, a bacterial cellulose producer previously isolated in the laboratory [45], was grown on the Hestrin and Schramm (HS) medium, containing 20 g/L glucose, 20 g/L peptone, 10 g/L yeast extract, 1.15 g/L citric acid, 6.8 g/L Na_2HPO_4, pH 6. The cultures were statically incubated at 25–28 °C for 7 days. After that time, bacterial cellulose membranes generated in the air/liquid interface of the culture media were harvested, rinsed with water and incubated in 1% (w/v) NaOH at 70 °C 18 h. Then, the BC membranes were thoroughly washed in deionized water until neutrality was reached. Membranes were mechanically disrupted with a blender and homogenized (Homogenizing System UNIDRIVE X1000) to obtain a BC paste containing a suspension of BC fibres. The amount of BC was determinated by drying samples of known weight at 60 °C until constant weight.

2.2. Expression and purification of SamLPMO10C

Escherichia coli BL21 star (DE3) harvesting pET11/SamLPMO10C [44] was cultured in LB medium supplemented with 50 μ/mL kanamycin at 37 °C, and induced by 0,5 mM isopropyl β-D-1-thiogalactopyranoside (IPTG) at O.D. 600 nm = 0.8. After cultivation at 21 °C for 18 h, cell pellets were collected by centrifugation and resuspended in 50 mM Tris-HCl pH 7. Cells were lysed using PANDA GEA 2000 homogenizer at 800 bar. Soluble fraction of the cleared cell extracts were mixed with 5% (w/v) Avicel® PH-101 (Fluka) with gentle rotary shaking for 1 h at 4 °C. Following, samples of SamLPMO10C were purified by polysaccharide-binding as described previously [44], with some modifications: to collect bound proteins, a centrifugation of 5 min at 14,000 × g was used to separate the pellet of insoluble polysaccharides with adsorbed enzymes. The pellets were sequentially washed 3 times with fresh buffer and centrifuged to remove non-specific protein binding. Pellets were washed with 3 volumes of 1 M glucose, for 30 min each, at 4 °C with gentle rotary shaking in order to elute adsorbed enzymes. Then, samples were centrifuged at 14,000 × g for 5 min to separate supernatants (with eluted SamLPMO10C) from pellet. Homogeneity of samples were analysed by sodium dodecyl sulphate polyacrylamide gel electrophoresis (SDS-PAGE).

2.2.1. Copper saturation

Purified SamLPMO10C (Uniprot, A3KKC4) was saturated with copper by incubation with a 4-fold molar excess of $CuSO_4$ for 30 min at room temperature as described elsewhere [40]. Excess copper and glucose were removed by desalting the proteins using a PD-10 desalting columns (GE Healthcare) equilibrated with 20 mM MES buffer, pH 5.5. The concentration of desalted Cu^{2+} - saturated SamLPMO10C was measured with NanoDrop® ND-1000 (NanoDrop Technologies, Inc), using an extinction coefficient (ε) at 280 nm of 75.775 M_1 cm_1. The enzyme solution was stored at −20 °C before used.

2.2.2. LPMO activity

Standard reactions were carried out by mixing 1% (dry weight) of substrate with 5 μM of Cu^{2+} - saturated SamLPMO10C, 2 mM ascorbic acid and 20 μM of H_2O_2 if necessary. Reactions were performed in 50 mM of ammonium acetate pH 5.5 with PASC (Phosphoric Acid Swollen

Cellulose) and H_2O_2, and BC, and incubated at 50 °C with shaking for 72 h and 24 h, respectively. PASC was obtained from crystalline cellulose Avicel ® PH-101 (Fluka) treated with 70% of H_3PO_4 according to Wood [46], using centrifugation for the sedimentation of the cellulose instead of decantation during the washing process. Control reactions without LPMO were run in the same way. All reactions were performed in duplicates at least three times. Soluble fractions generated in the degradation reactions were analysed by matrix-assisted laser desorption/ionization time of flight mass spectrometry (MALDI-TOF MS) for the analysis of oxidized products. Reaction samples (3 μl) were mixed with 7 μl of acetonitrile. 1 μl of this solution was mixed with 1 μl of matrix solution (10 mg/ml of 2,5-dihydroxybenzoic acid dissolved in acetonitrile–water [1:1, vol/vol], 0.1% [wt/vol] trifluoroacetic acid)0.1 μl of the mixture was spotted in duplicated onto the MALDI-TOF MS plate and allowed to dry before the analysis. Positive mass spectra were collected with a 4800 Plus MALDI TOF/TOF (ABSciex 2010) spectrometer with an Nd:YAG 200-Hz laser operated at 355 nm.

2.3. Cellulase cocktail activity

Enzymatic product MetZyme® BRILA™ (cellulase cocktail C2) was kindly supplied by MetGen Oy (Finland) [47]. Reducing sugars resulting from glycosil hydrolase activity were quantified by the DNS reagent method [48]. Standard assays were performed at 50 °C in 50 mM potassium acetate buffer at pH 5. Solid material was removed by centrifugation at 12.000 × g for 5 min and cleared supernatant was analysed. One unit of enzymatic activity was defined as the amount of enzyme that releases 1 μmol of reducing sugar equivalent per min. A standard curve of glucose was used to calculate activity units. All determinations were made in triplicate at least two times.

2.4. Enzymatic preparation of bacterial cellulose nanocrystals (BCNC)

Enzymatic hydrolysis of the BC paste was run using the enzymes SamLPMO10C and the cellulose cocktail C2. Bacterial cellulose paste (1% dry weight) was mixed with Cu^{2+} - saturated SamLPMO10C and 2 mM ascorbic acid in 50 mM ammonium acetate pH 5.5. The mixture was kept in 50 °C for 24 h. Then, 12.5 U g^{-1} odp (oven-dried pulp) of C2 was added and the mixture was incubated at 60 °C for 18 h. For control reaction, the same dried weight of bacterial cellulose paste was incubated in all the buffer components at the same conditions. All reactions were incubated with shaking in a water bath. Hydrolysis was stopped by heating up the reaction to 100 °C for 10 min. The obtained suspensions were homogenized by ultrasonication (80 W, 0.8 s) in a Labsonic 1510 sonicator (B.Braun) for 5 min and kept at 4 °C.

2.5. Characterization of BCNC

2.5.1. Scanning electron microscopy (SEM)

Water suspensions of BCNC were analysed by SEM (JSM 7100F) using a LED filter. Samples were graphite coated using a Vacuum Evaporator EMITECH K950X221. EDS analysis was carried out to verify their chemical composition. The diameter of the fibres was measured using the ImageJ software.

2.5.2. Transmission electron microscopy (TEM)

Suspensions of BCNC were negatively stained with 2% uranyl acetate, after dropping them on a Cu grid covered with formvar and a thin carbon film, and allowed to dry at room temperature. The diameter and length of BCNC were obtained using a transmission electron microscope (TEM) model JEOL 1010. Images were taken at an accelerated voltage of 80 kV. The length (L) and width (D) were determined from at least 100 measurements using the ImageJ software.

2.5.3. X-ray diffraction

X-ray diffraction patterns of dried samples of BCNC were obtained with a PANalytical X'Pert PRO MPD Alpha1 powder diffractometer. The samples were analysed at the radiation wavelength of 1.5418 Å and scanned from 2 ° to 50°, 2θ range. Samples were fixed over a zero background Silicon single crystal sample holder (pw1817/32), and the ensembles were mounted in a PW1813/32 sample holder. The same Silicon holder was used to measure all the replicates of each sample. Eq. (1) [49] was used to calculate the crystallinity index (CI) of bacterial cellulose:

$$CI(\%) = \frac{I_c - I_{am}}{I_c} \times 100 \quad (1)$$

where I_c is the maximum intensity of the lattice diffraction and I_{am} is the height of the intensity at the minimum at 2θ between 18 ° and 19 °, which corresponds to the amorphous part of cellulose.

2.6. Zeta potential

BCNC suspensions and BC were previously diluted in distilled water to a 1:5 and 1:10 sample:water ratio (v/v), respectively. Zeta potential was then measured in a Zetasier NanoZS (Malvern Instruments, UK), in triplicate.

2.7. Particle size determination

2.7.1. Light scattering (LS)

The particle size of BCNC was measured by laser diffraction in the range of 0.375–20000 μm in a Particle Size Analyzer (Beckman Coulter LS 13320), using the Micro Liquid Module in aqueous suspension and Fraunhofer optical model.

2.7.2. Filtration

After the enzymatic hydrolysis was complete, the final reaction containing the BCNC was filtered by several filters with a decreasing diameter pore size (50 μm, 6 μm, 3 μm, 0.4 μm and 0.2 μm, Nangtong FilterBio Membrane Co., Ltd). Then, the filters were left to dry at 80 °C for 24 h and the retained biomass was weighted.

2.8. Thermogravity analysis (TGA)

The thermal stability of BCNC was measured by TGA on TGA/SDTA851^e (Mettler Toledo). The experimental conditions were as follows: the test sample was heated at a rate of 10 °C / min to a maximum of 700 °C in nitrogen inert medium at a flow rate of 50 mL/min. The weight of the dry sample was about 1 mg.

2.9. Composites formation and characterization

Eucalyptus/BCNC nanocomposites were obtained by a modification of the solving casting technique [50,51]. BCNC were added at different concentrations to preformed 10% (w/v) eucalyptus sheets on a 0.2 μm pore size filter while applying vacuum. Finally, they were left to dry at room temperature for 72 h under pressure. Water permeability was measured by the water drop test (WDT) according to TAPPI standard T835 om-08. The WDT involved placing a drop of deionized water on the surface of paper and recording the time needed for complete absorption, which was signalled by vanishing of the drop specular gloss. Ten measurements per sample were made and averaged. Grease resistance was determined by the standard UNE 5707174, where silica sand was placed on the composite before dyed turpentine was added, and the time needed to penetrate it was counted. Atomic force microscopy (AFM) – Peak Force (PF) Quantitative Nanomechanical Mapping (QNM) mode – was used to determine the tensile properties. Measurements were done with an Antimony (n) doped Si from Bruker, model RTESPA-525 with the characteristics: nominal tip radius 8 nm, cantilever length of 25 μm, resonant frequency 375–675 kHz.

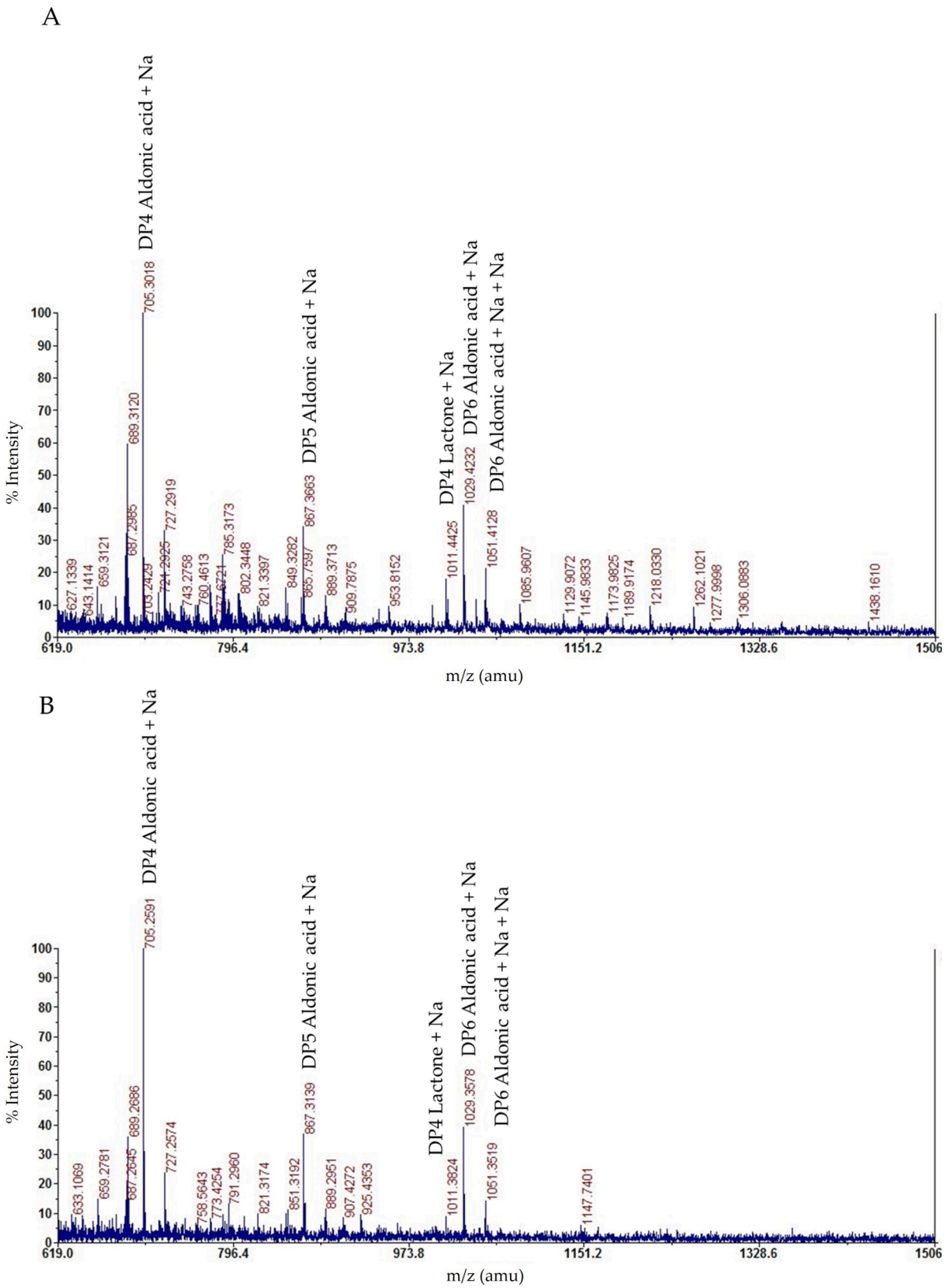

Fig. 1. MALDI-TOF MS analysis of soluble oxidized products from **(A)** PASC and **(B)** BC.

2.10. Statistical analysis

All determinations were performed after two replicas. In the case of enzyme activity, two replicas of triplicates (six determinations per sample) were measured. Experimental data were expressed as means ± standard deviations and were analysed statistically by the paired Student's *t*-test method and analysis of variance (ANOVA) if there were more than two groups in STATGRAPHICS Centurion XVIII software

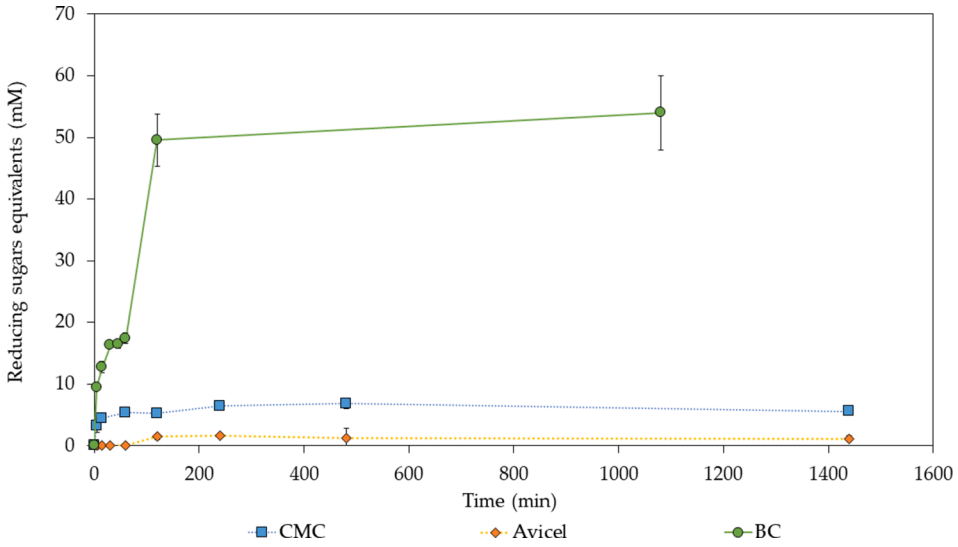

Fig. 2. Activity per mM reducing sugars equivalents of the industrial cellulolytic cocktail over time on different substrates: CMC (squares line), Avicel (rhombus line) and BC (dots line).

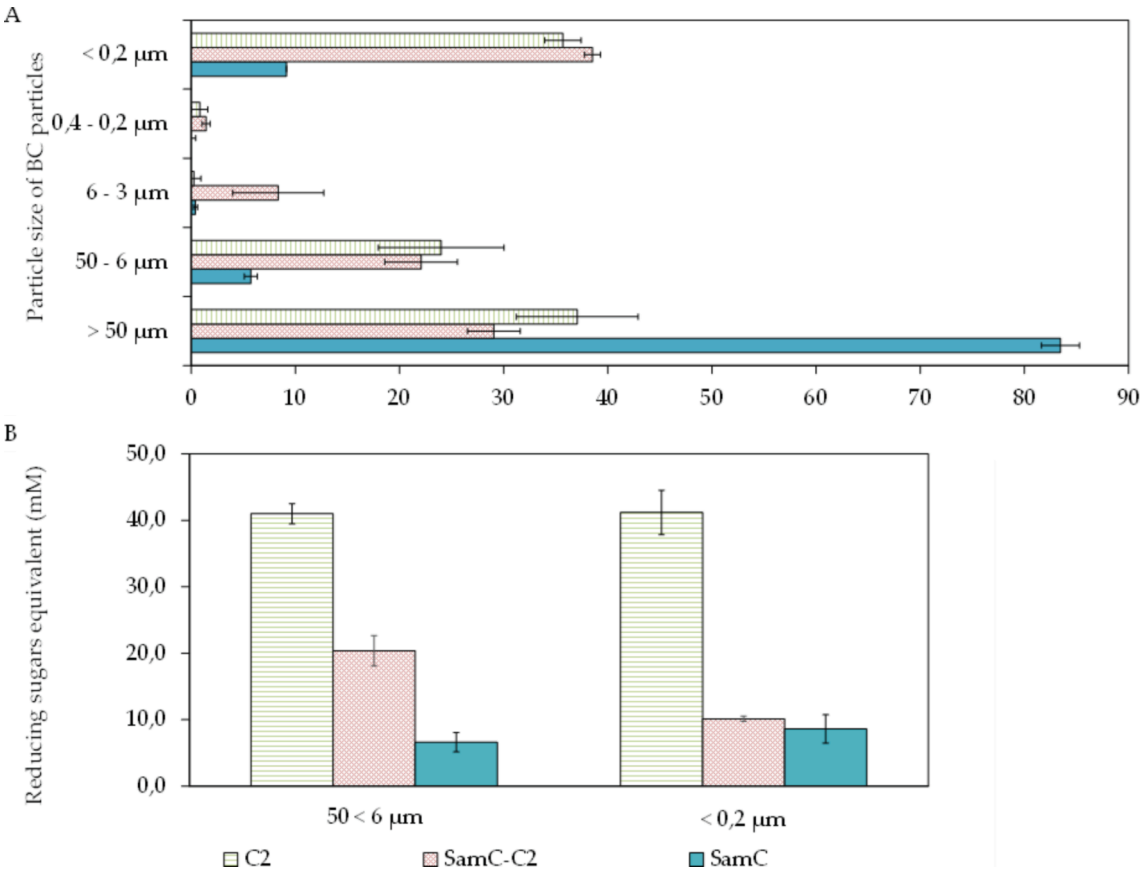

Fig. 3. BCNC length distribution by filtration **(A)** and reducing sugars content **(B)** after the enzymatic treatment.

(Statgraphics.Net, Madrid). Scheffe's multiple range test was used to detect differences among mean values. A value of $p \leq 0.05$ was considered statistically significant. Homogeneity of variance for all samples was tested with Bartlett's test. Residues normal distribution was assumed after performing the Shapiro-Wilk test.

3. Results and discussion

3.1. SamLPMO10C and cellulase activity onto bacterial cellulose

Prior to bacterial cellulose nanocrystals obtention by enzymatic hydrolysis, the activities of purified SamLPMO10C, hereinafter SamC, and cellulase cocktail C2 activities were tested. SamC standard reactions were performed with PASC, routinely considered as the preferred

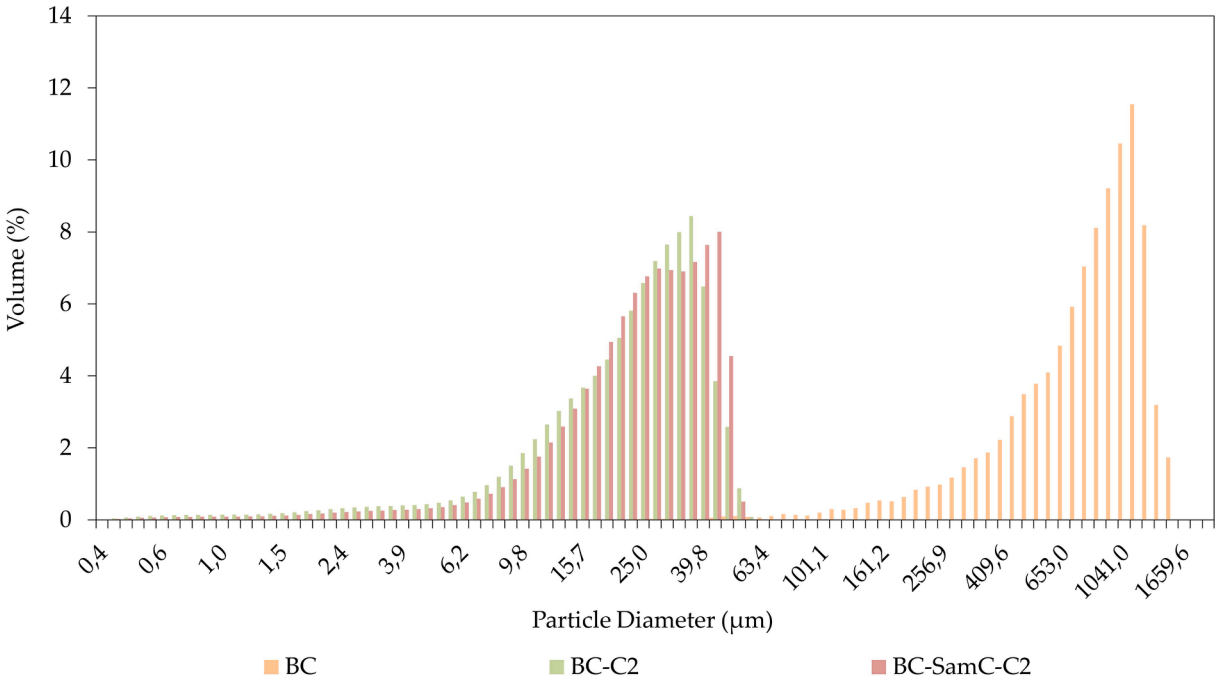

Fig. 4. Particle size distribution of native BC and after enzymatic treatments.

substrate of cellulose active LPMOs [44], and BC. MALDI-TOF MS detection of the soluble oxidized products from SamC activity is shown in Fig. 1. The analysis of the reaction products revealed that, under the reaction conditions used, SamC was active in both substrates, generating oxidized cellooligosaccharides with different degrees of polymerization (DP), of 4–7 in the case of PASC, and 4–6 for BC, in accordance with previous results from the research group [44,52]. In all cases, the peak assignment was in agreement to the size of C1-oxidized fragments from released aldonic acid oligosaccharides.

Glycosyl hydrolase activity of C2 was measured by the reducing sugars method on three crystalline cellulosic substrates: soluble cellulose (CMC, carboxymethyl cellulose), insoluble microcrystalline cellulose (Avicel) and BC, the most crystalline among them. As shown in Fig. 2, the amount of reducing sugars increased over time until a threshold was reached after 2 h of incubation, indicating, cellobiohydrolase activity. However, the activity for BC was notably higher indicating that, likewise SamC, C2 had preference for crystalline substrates as BC, the source of nanocrystals of this work.

3.2. *Bacterial cellulose nanocrystals obtention and size distribution*

To obtain BCNC, the BC paste was first treated with SamC and then with cellulases C2. Reactions with only SamC or C2 were also run in parallel. Mass spectrometry analysis were performed to detect soluble oxidized products from SamC activity onto BC, as well as to discard LPMO activity from the commercial cocktail C2 (Fig. A1). The particle size distribution of the enzymatically treated samples was attempted by filtering them through a series of membranes of decreasing pore diameter. As can be seen in Fig. 3**A**, there was a significant shift towards lower fibre sizes after cellulase hydrolysis of BC, in both cases, with and without prior action of SamC. However, more than 80% of the biomass of BC treated only with SamC is retained by 50 μm, while only 37% of the biomass subjected to the action of cellulases exceeds that size, corroborating that cellulases are the main responsible for the digestion of BC. Considering particles < 50 μm, the yield of BCNC obtained by C2 digestion would be of 62.9%, whereas for the pretreatment of SamC followed by C2 cellulase activity would increase it up to 70.9%. Interestingly, with the combined SamC-C2 treatment, more particles between 3 μm and 400 nm were obtained than with only C2 digestion [57], besides that for the bigger fractions all bars are smaller. These results would suggest that with LPMOs the obtained BCNC would have a larger length than those obtained with cellulases alone, which is in disagreement with the generally accepted role of auxiliary activity of LPMO [43,44,53]. This enzyme is thought to make crystalline cellulosic substrates, as BC, more accessible to the glycoside hydrolases, boosting their activity [44]. However, the reported pattern was found again after measuring the reducing sugars of the filtrates 50 < 6 μm and < 200 nm of each treatment (Fig. 3**B**). The value of reducing sugars after the combined SamC-C2 treatment was higher than those presented by the samples treated only with SamC, indicating that cellulase digestion has been effective. When comparing the two filtrates (50 < 6 μm and < 200 nm) after C2 treatment, there are no apparent differences between them, which could mean that the obtained particles are of small size, with a low degree of polymerization. Nevertheless, for SamC-C2 treatment, the value of reducing sugars is more elevated in the 50 < 6 μm filtration than in the < 200 nm one, reinforcing the prior hypothesis that a previous treatment with SamC before the cellulases digestion resulted in larger particles. Moreover, recent studies have reported severe impeding effects of C1-oxidizing LPMOs on the activity of reducing-end cellobiohydrolases [54]. Even though not knowing the underlying mechanism of this impeding effect, we justify the use of SamLPMO10C for the dispersive properties of the obtained BCNC.

Fig. 4 shows the results of laser diffraction (LS) technique by light scattering, which enabled determination of particle size, based on the diffraction of incident light on a sample. Again, it is clearly visible the effect of C2 onto the BC. In both treatments, SamC-C2 and C2, a shift towards smaller sizes particles could be observed. However, it can be noticed that particles obtained after SamC-C2 treatment had higher percentages of higher diameters than those obtained without previous SamC treatment. The high amount of particles of size greater than 2 μm observed in Fig. 4 could be easily attributed to agglomeration [55]. Similar results were observed by other authors who explain this tendency to agglomerate with presence of strong OH^- intermolecular bonds occurring in cellulose [51]. It should be noted that this technique assumes that the analysed particles are spheres [12], and cellulose nanocrystals are rod-like particles, not spherical. Nevertheless, these results corroborated the effect of the combination of SamC and cellulases treatment on the size of BCNC found by the filtration method.

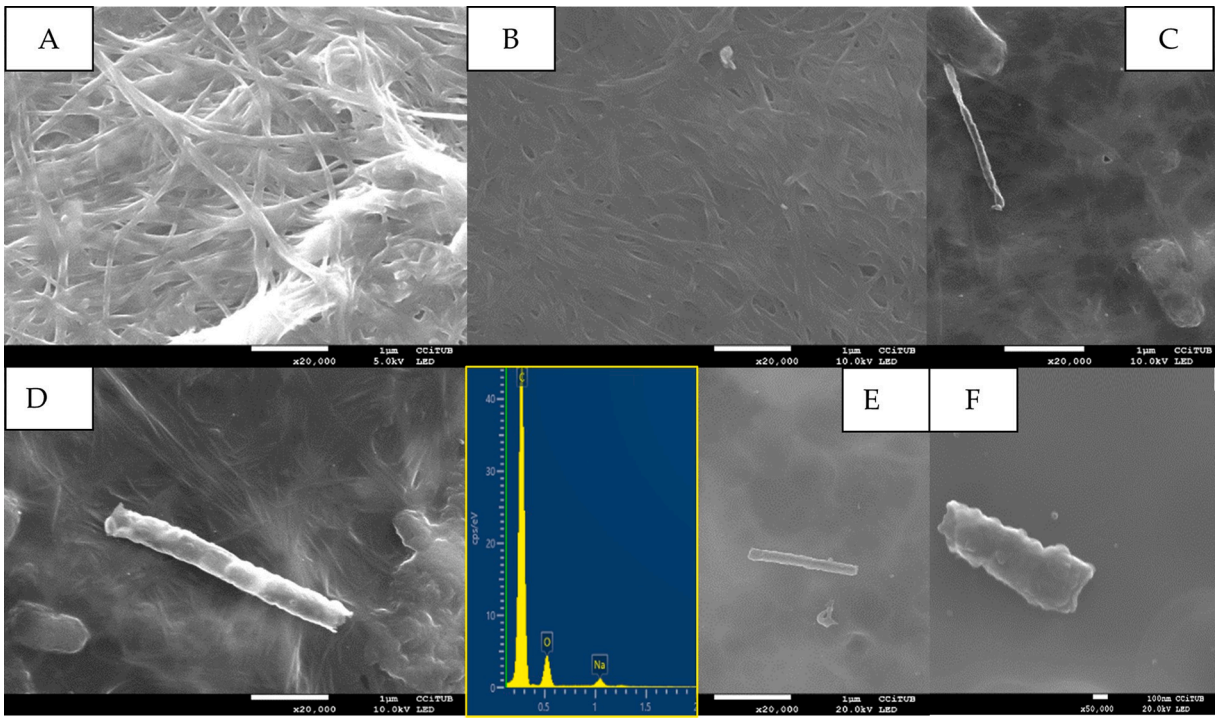

Fig. 5. Electron microscopy images obtained by SEM: BC **(A)**, BC-SamC **(B)**, BCNC **(C-F)**. The insert in (E) represents the energy dispersive X-ray spectrometer (EDS) spectrum of BCNC.

3.3. BCNC characterization

3.3.1. Morphology

Electron microscopy images of BCNC are shown in Fig. 5 and Fig. 6. Scanning electron microscopy (SEM) pictures of the native BC and oxidized BC by SamC (Fig. 5**A, B**) show the typical reticulated structure consisting of ultrafine cellulose fibrils with a diameter of about 50 – 70 nm and a length exceeding 20 μm, consistent with previous results [3,56]. Treatment with SamC did not noticeably change the cellulose structure, in agreement with other authors who oxidized BC with SamLPMO10C [52] or 2,2,6,6-tetramethyl-1- piperidinoxyl (TEMPO) [57]. In images of samples of BC enzymatically treated (Fig. 5**C-F**), rod-like structures compatible with BCNC were observed, with a length (L) in the range 80 nm – 2 μm. Energy Dispersive X-ray spectroscopy (EDS) confirmed that these structures were composed of cellulose.

Transmission electron microscopy (TEM) micrographs of BCNC allowed a more detail analysis (Fig. 6**A**). The observed flat, rod-like particles had a small number of laterally associated elementary crystallites, usually from 3 to 5, as it has been previously described [28,58]. In TEM negatively stained preparations (Fig. 6**B-G**), the accumulation of stain around the narrower parts of the nanocrystals suggested an alternation of narrow and wide parts along the BCNC, indicating that they would have a ribbon-like shape and that a homogeneous twist occur [59]. This twist (Fig. 6**H-I**), which is rarely directly observed [59], is especially clearly observed in well-dispersed ribbon-shaped bacterial cellulose [60], even if it is not clear its origin. It could be attributed to a rotational movement of bacteria or enzyme complexes or to the chiral nature of cellulose, or a combination of both [59]. BCNC had a length ranging from 80 to 2000 nm and a width ranging from 3 to 12 nm, which represented an average length (L) and width (D) of 711 ± 154 nm and 9 ± 5 nm, respectively. These sizes are in line with those reported for BCNC obtained by acid hydrolysis by others. [61-65]. BCNC are usually larger in dimension compared to those obtained from vegetal cellulose as wood and cotton [66,67], hence there are lower fractions of amorphous regions that need to be cleaved resulting in the production of larger nanocrystals [11]. Moreover, these dimensions lead to a higher ratio of length to diameter (L/D). The aspect ratio L/D of the BCNC here obtained was 80.1. The geometrical aspect ratio of cellulose nanocrystals is very important in defining their reinforcing capability in polymer matrices. Generally, nanocrystals exhibiting a ratio L/D greater than 13 results in improved reinforcement properties of the final polymer nanocomposites [11,68].

3.3.2. Crystallinity

Regarding chemical structure, XRD patterns were measured. Fig. 7 showed diffraction peaks at 2θ angles around 18.5 θ and 22.7 θ, corresponding to the typical profile of cellulose in crystalline form [69]. The estimated degree of crystallinity index (Eq. (1)) of the native BC was 97% and 95% for oxidized BC. For BCNC, obtained by SamC-C2 treatment, or only by C2 treatment, the crystallinity index barely changed, with a value of 85%. It should be noted that BC is one of the most crystalline cellulosic substrates [52], and in this work an enzymatic digestion has been performed. Consequently, some of the BC could have been completely hydrolysed, reflected in this slight decrease in crystallinity. In fact, it has been described that severe hydrolysis conditions can result in a likely change in the orientation of the cellulose chains [70]. However, the obtained BCNC displayed high crystallinity, even higher than BCNC obtained by acid hydrolysis [70-72], suggesting that the enzymatic treatment did not modify characteristics as mechanical strength and interfacial properties of the cellulose fibre [73].

3.3.3. Dispersion stability

The zeta potential was measured to evaluate the dispersion stability of BCNC suspensions in water (Fig. 8), where less negative the values are, better is the stability [74]. Interestingly, suspensions of BCNC where SamC was applied presented a zeta potential modulus much higher than suspensions of BCNC obtained without SamC treatment (-6.5 mV and −21.4 mV, respectively), indicating that SamC treatment was necessary for their stability. These results suggested that after SamC mediated oxidation, the negatively charged carboxylic groups would promote electrostatic repulsion and prevent the aggregation of the nanocrystals. CNC obtained by sulphuric acid hydrolysis often acquire a negatively

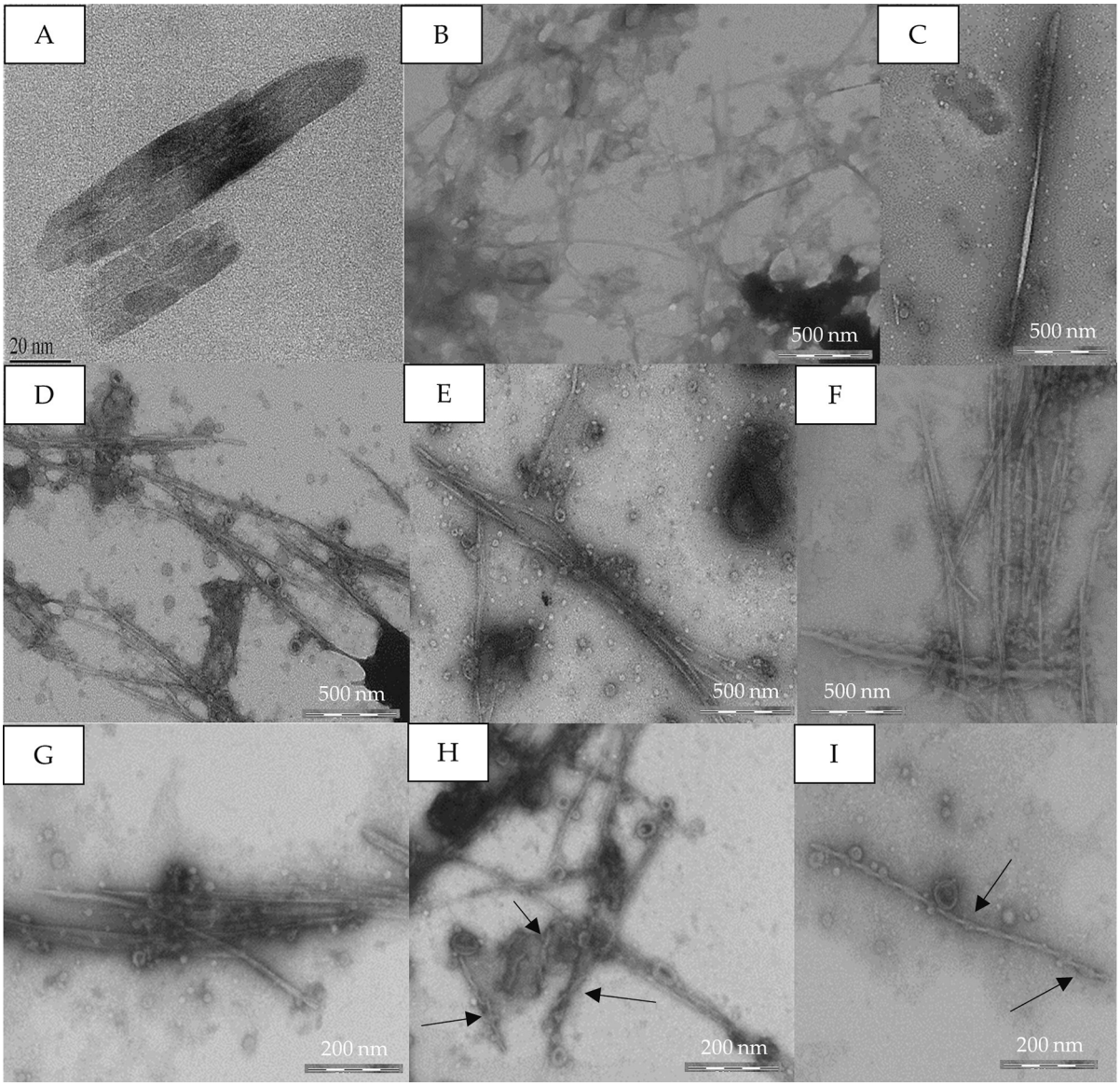

Fig. 6. Electron microscopy images of BCNC obtained by TEM **(A)** and negative stain TEM **(B-I)**. The arrows in (H) and (I) highlight the twist.

charged surface which promotes uniform dispersion in aqueous solution due to electrostatic repulsions [75]. However, even if this sulfonation results in a highly stable colloidal suspension, the obtained CNC are prone to have a lower thermal stability as compared to the native cellulose [76]. On the other hand, without these negative charges, CNC are prone to aggregate because of their strong hydrogen bonding between surface hydroxyl groups [64]. Consequently, this uniform dispersion provided by sulphate groups is a challenge when more environmentally friendly treatments, as the enzymatic ones, are applied. One of the more efficient pretreatments to cellulose is the oxidation mediated by TEMPO, as some authors have reported in the case of the obtention of oxidized nanofibrillated bacterial cellulose [57]. Alternatively, LPMOs have proved to contribute to a more sustainable production of cellulose nanofibrils [41,52], and they could also have a key role, as oxidative enzymes, in giving dispersion stability to BCNC obtained exclusively by enzymatic treatment.

3.4. Thermostability

Thermal stability of cellulose often is drastically changed due to acid hydrolysis during the process of cellulose nanocrystals obtention [76]. Therefore, it is important to establish whether the enzymatic treatments have a similar effect. For this purpose, the thermal degradation profiles of BC and BCNC were assessed by thermogravimetric analysis (TGA). Fig. 9 represents the three mass loss events that can be observed during TGA: the first event corresponds to the evaporation of residual water, while the second is characterized by a series of degradation reactions of cellulose [70,77]. This major degradation step is, though, associated with a high loss of mass of cellulosic material, which is characterized by the onset temperature (T_O, the temperature at 5% weight loss). The third thermal event is related to the unburnable residue. As stated in Table 1, a maximum decomposition point was observed for BC and BC-SamC around 140 °C, even if they had slightly different onset temperatures. Interestingly, enhanced thermal stability was noticed for BCNC, as the maximum degradation rate was registered at a higher temperature: 211,3 and 237,1 °C for those obtained with C2 only and SamC and C2, respectively. These differences could be related to the different defibrillation conditions [78,79]: in comparison with BCNC, BC and BC treated with SamC have a more compact structure for the same weight, leading to a better heat transference and therefore to a higher degradation rate. BCNC with high thermal stability can be used, for instance, for nanocomposites preparation where the polymers blending process

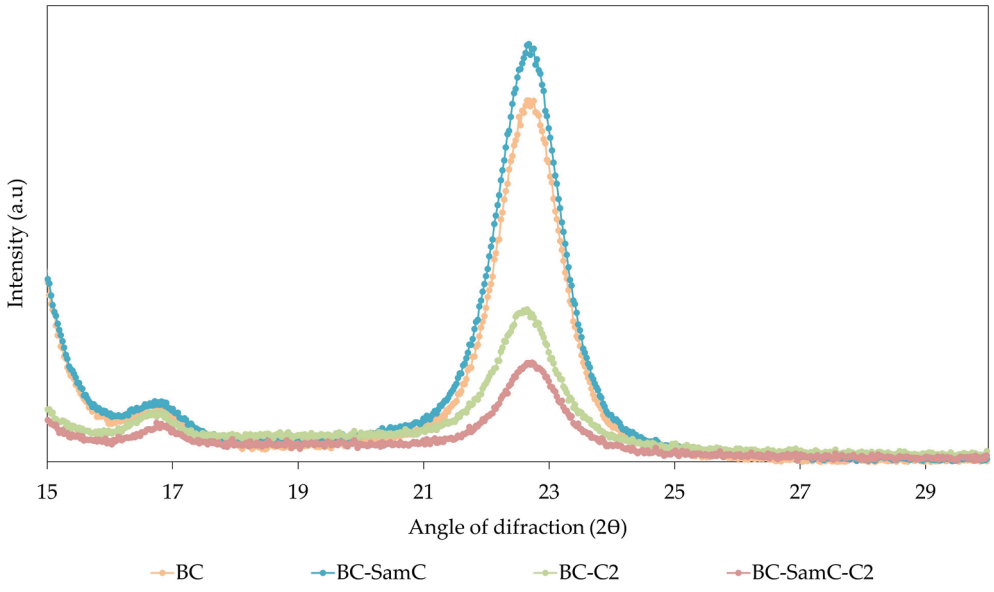

Fig. 7. XRD pattern of BC, BC-SamC and BCNC (BC-C2 and BC-SamC-C2).

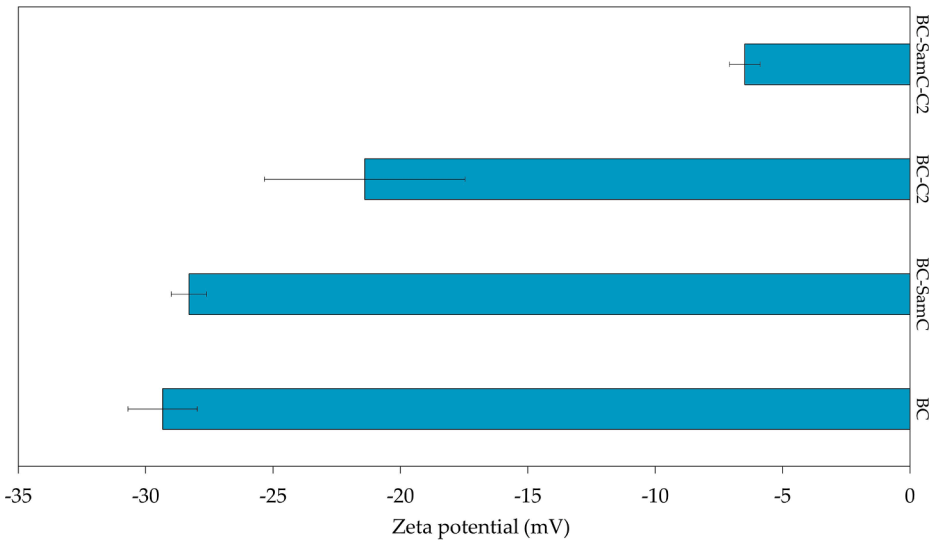

Fig. 8. Results from zeta potential of suspensions of BC, BC treated with SamC (BC-SamC) and with C2 cellulases (BC-C2 and BC-SamC-C2).

requires high temperature.

3.5. *Eucalyptus /BCNC nanocomposites*

When a polymer is reinforced with a nanomaterial, a polymer nanocomposite is obtained. The nanometric size and the increased surface area of the reinforcing material provides this new nanocomposite unique properties. Their incorporation in many polymers, even at very low volume fractions, can significantly improve the mechanical performance, thermal stability, and barrier and optical properties due to its elevated crystallinity and better interfacial interactions, probably due to high interfacial interactions [5,80]. For this purpose, to assure a good adhesion between the coating and the cellulosic sheet, in this study BCNC were physically incorporated in different doses to prepared 10% (w/v) eucalyptus sheets by casting and water evaporation, one of the most common and effective techniques to produce nanocomposite films on a laboratory scale [11]. As described by other authors, CNC obtained without sulphuric acid often reaggregate [64]. For this reason, CNC are usually chemically modified to improve their dispersion [12]. Nevertheless, the BCNC obtained in this study were negatively charged due to SamC treatment, and as stated by the determination of z potential, they were well dispersed. Overmore, their ratio L/D indicated a high reinforcing capability. Consequently, the obtained composites were homogeneous, no holes or big agglomerates were present in comparison to those coated with BCNC obtained without oxidation. According to literature, Xiang et al. [81] and Yuan et al. [82] proved that getting a homogeneous distribution of BCNC matrix is a key for successfully reinforcing paper in the paper industry. In further studies, these BCNC could serve as a matrix for active compounds immobilization, and the resultant nanocomposites could have special properties, as antimicrobial, antioxidant or catalytic ones [83-86]. They could also provide functionality to biodegradable packages and ability to control microbial population in the food, in the industry of food packaging [12].

3.5.1. *Water permeability*

All the nanocomposites showed an increased water impermeability in comparison to the eucalyptus sheet (Fig. 10). Interestingly, water retention time reached a threshold over 7 min at 4% BCNC addition.

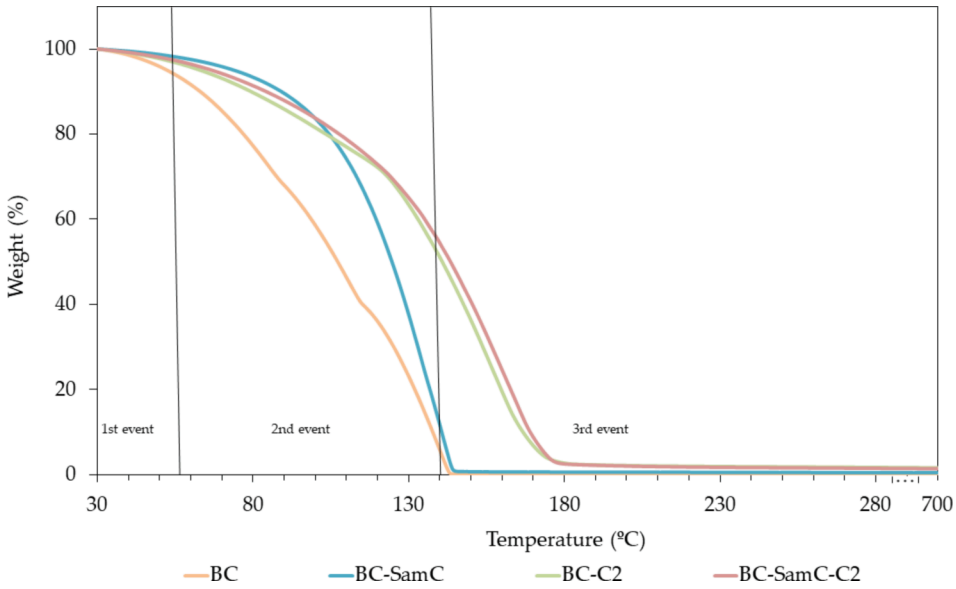

Fig. 9. Thermogravimetric curve of native BC, BC-SamC and after enzymatic treatments with cellulases (BC-C2) and SamC and cellulases (BC-SamC-C2).

Table 1
TGA results for BC, BC-SamC and BCNC after enzymatic treatments with cellulases (BC-C2) and SamC and cellulases (BC-SamC-C2).

	Onset temperature degradation (T_O) (°C)	Maximum degradation temperature (Td) (°C)
BC	63	141.7
BC-SamC	89.3	142.7
BC-C2	85.7	211.3
BC-SamC-C2	107	237.1

This effect can be easily attributed to the low hygroscopicity of highly crystalline BCNC [64]. The water transmission preferentially occurs through the amorphous areas of cellulose and their absence leads in an increase of the time that the water drop is retained on the surface of the nanocomposite. Overmore, the negative charged BCNC contribute to this decrease in water permeability.

3.5.2. *Oil impermeability*

Regarding barrier properties, a threshold was reached again at 4% of BCNC addition. As shown in Fig. 11, from this concentration the nanocomposite was able to hold the trementine solution for more than 30 min, indicating that it was grease resistant. This enhancement in barrier properties is probably due to the reduction of eucalyptus sheets porosity [12]. According to other authors, the high aspect ratio aspect of BCNC would give this reinforcing effect, ensuring percolation, event at low loadings [80,87]. Materials with low permeability to moisture and oil are very much needed in food and biomedical packaging areas [88].

3.5.3. *Mechanical properties*

Loading of BCNC resulted in improved mechanical resistance. The

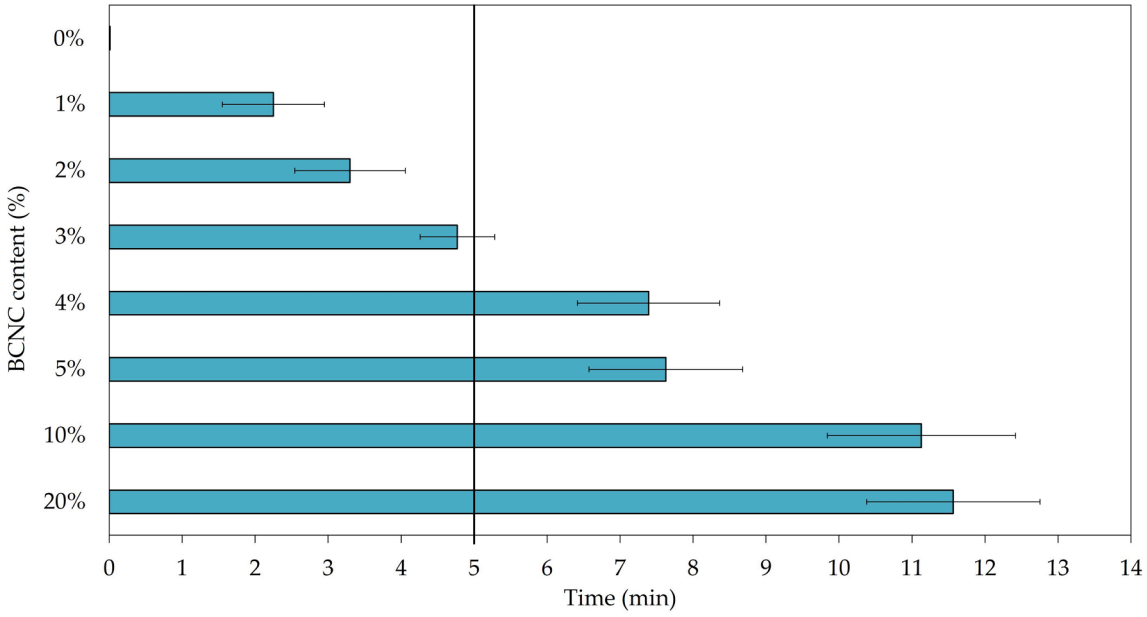

Fig. 10. Water drop test values of the BCNC-eucalyptus composites with different loadings of BCNC. The black line represents the 5 min threshold according to TAPPI standard T835 om-08.

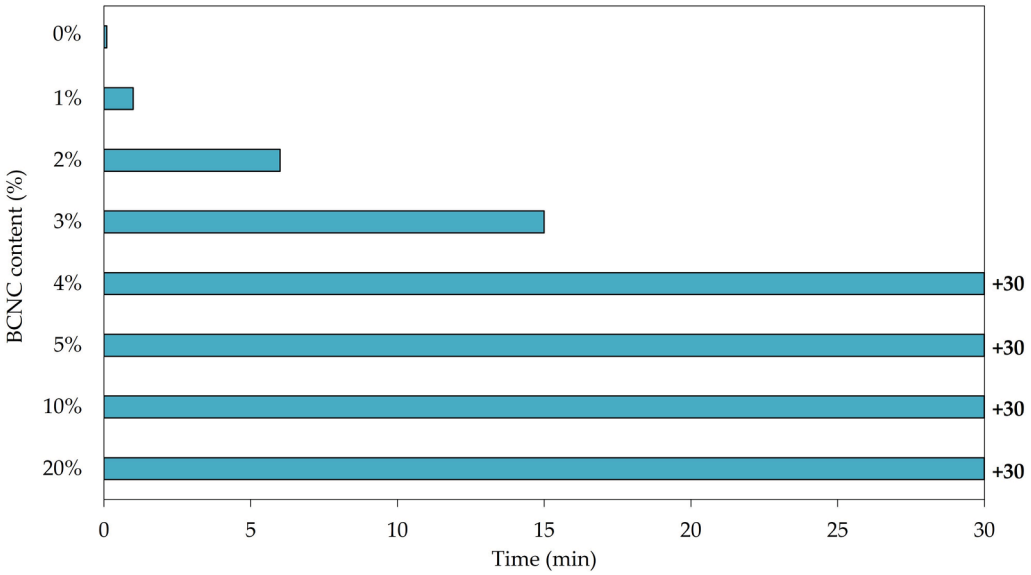

Fig. 11. Barrier properties to oil of the BCNC-eucalyptus composites with different loadings of BCNC.

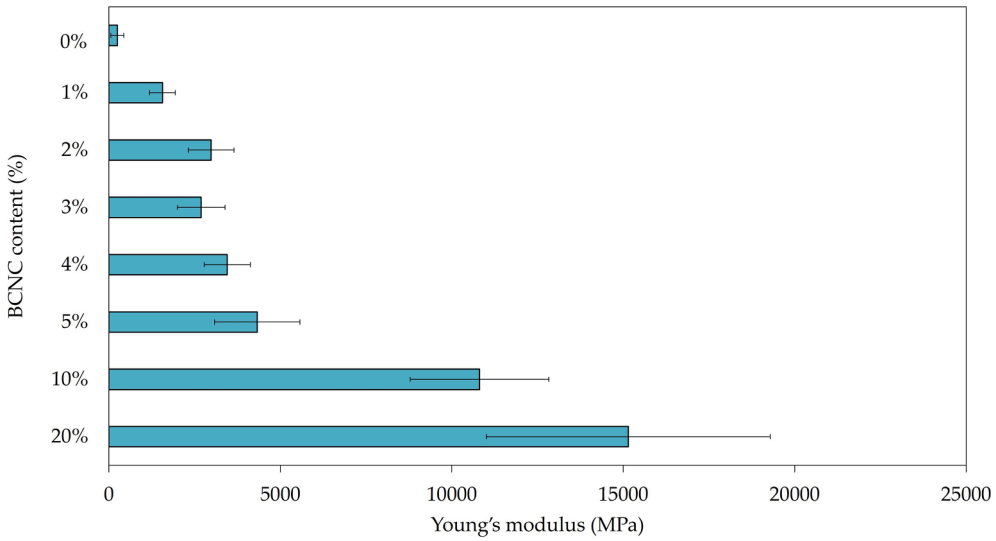

Fig. 12. Young's modulus parameters obtained for the tested composites with the addition of different BCNC loadings onto eucalyptus sheets.

highest values of Young's modulus (YM) were observed for composites with 20% loading of BCNC (Fig. 12). The addition of BCNC onto eucalyptus sheets lead to a increase of the yield strength, almost 15 times when BCNC were added at 20%, from 246.42 ± 190.1 MPa to 15.15 ± 4.1 GPa. However, in the literature is very often reported that composites with the smallest amount of filler are characterized by the highest values of strength parameters, resulting from their better dispersion [89-91]. Surprisingly, in our study, further increase of BCNC resulted in improvement of YM parameters, as it has been also recently described elsewhere [55,92].

4. Conclusions

In this work, bacterial cellulose nanocrystals have been obtained using a green procedure. A pretreatment with the enzyme SamLPMO10C, followed by digestion with a mixture of cellulases, led to the obtention of nanocrystals with high aspect ratio, high crystallinity index and excellent thermal properties. The oxidative action of LPMO generated negative charges on the cellulose chains on the surface of the nanocrystals that prevented aggregation and allowed good stability in an aqueous environment. Eucalyptus cellulose sheets coated with a low percentage of bacterial cellulose nanocrystals acquired water and oil impermeability and improved mechanical properties. The properties of the nanocrystals obtained by this enzymatic process make predictable a wide range of applications.

Funding

This work was financed by the Spanish Ministry of Economy, Industry and Competitiveness, grant CTQ2017-84966-C2-2-R, by the Pla de Recerca de Catalunya, grant 2017SGR-30, and by the Generalitat de Catalunya, "Xarxa de Referència en Biotecnologia" (XRB). C. Buruaga-Ramiro acknowledges an APIF predoctoral grant from the University of Barcelona.

Declaration of Competing Interest

The authors declare that they have no known competing financial

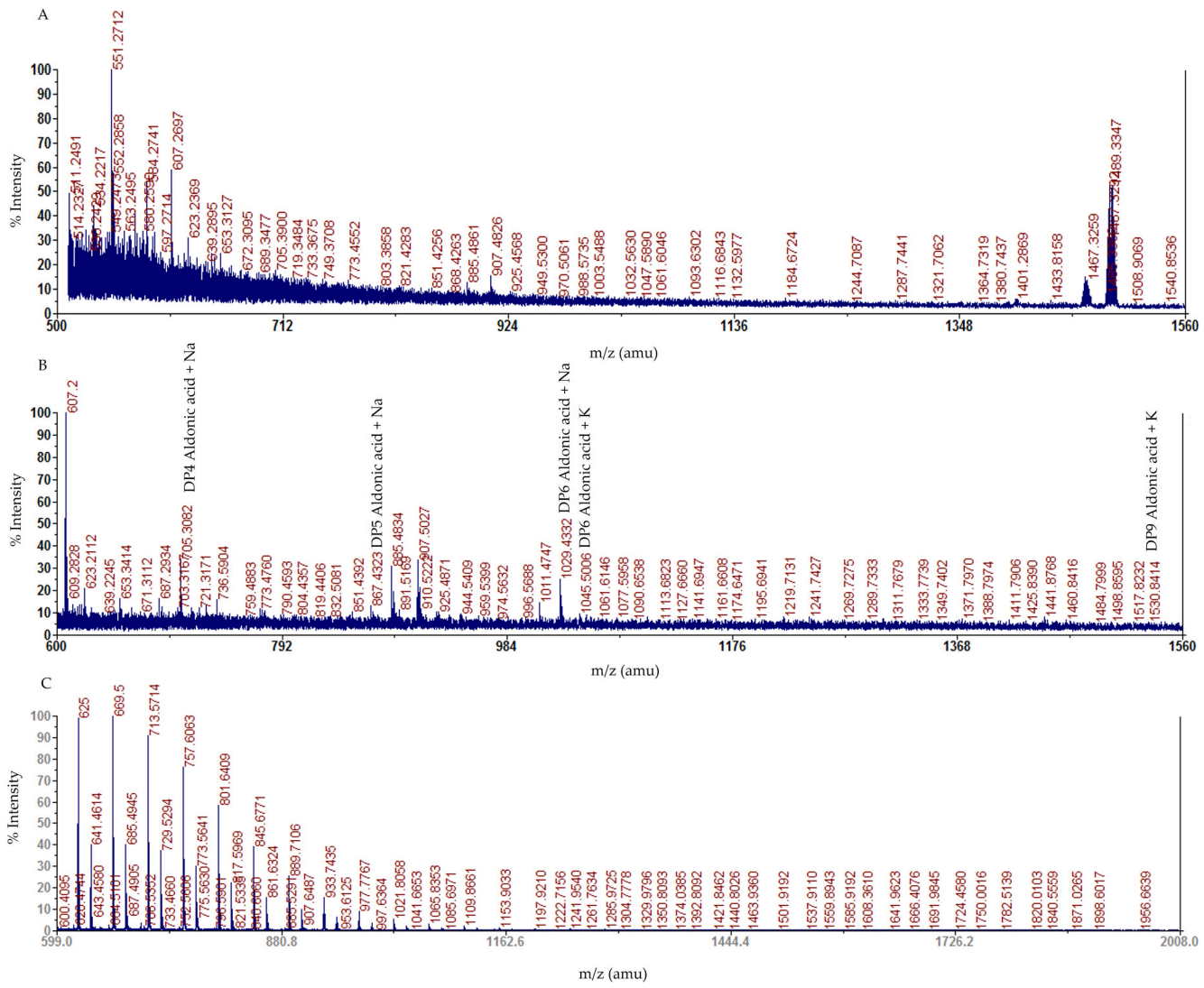

Fig. A1. MALDI-TOF MS analysis of soluble oxidized products from **(a)** BC negative control, **(b)** BC-SamLPMO10C and **(c)**, BC-SamLPMO10C-Cel.

interests or personal relationships that could have appeared to influence the work reported in this paper.

Acknowledgements

We thank the Serveis Cientifico-Tècnics of the University of Barcelona (CCiTUB) for technical support in: electron microscopy; X-ray diffraction; laser diffraction; TGA analysis and AFM, and Institut de Ciències de Materials de Barcelona (ICMAB-CSIC) for z potential measure. We are grateful to MetGen Oy (Finland) for supplying enzyme products. M. Vieiros is acknowledged for technical assistance.

Data availability

The raw/processed data required to reproduce these findings cannot be shared at this time due to technical or time limitations.

Appendix

References

[1] R.N. Tharanathan, Biodegradable films and composite coatings: Past, present and future, Trends Food Sci. Technol. 14 (2003) 71–78, https://doi.org/10.1016/S0924-2244(02)00280-7.

[2] A. Dufresne, Comparing the mechanical properties of high performances polymer nanocomposites from biological sources, J. Nanosci. Nanotechnol. 6 (2006) 322–330, https://doi.org/10.1166/jnn.2006.906.

[3] C. Buruaga-Ramiro, S.V. Valenzuela, C. Valls, M.B. Roncero, F.I.J. Pastor, P. Díaz, J. Martínez, Bacterial cellulose matrices to develop enzymatically active paper, Cellulose 27 (2020) 3413–3426, https://doi.org/10.1007/s10570-020-03025-9.

[4] C. Zinge, B. Kandasubramanian, Nanocellulose based biodegradable polymers, Eur. Polym. J. 133 (2020), 109758, https://doi.org/10.1016/j.eurpolymj.2020.109758.

[5] J. George, S.N. Sabapathi, Cellulose nanocrystals: Synthesis, functional properties, and applications, Nanotechnol. Sci. Appl. 8 (2015) 45–54, https://doi.org/10.2147/NSA.S64386.

[6] M. Ghorbani, L. Roshangar, J. Soleimani Rad, Development of reinforced chitosan/pectin scaffold by using the cellulose nanocrystals as nanofillers: An injectable hydrogel for tissue engineering, Eur. Polym. J. 130 (2020), 109697, https://doi.org/10.1016/j.eurpolymj.2020.109697.

[7] S.J. Eichhorn, A. Dufresne, M. Aranguren, N.E. Marcovich, J.R. Capadona, S. J. Rowan, C. Weder, W. Thielemans, M. Roman, S. Renneckar, W. Gindl, S. Veigel, J. Keckes, H. Yano, K. Abe, M. Nogi, A.N. Nakagaito, A. Mangalam, J. Simonsen, A. S. Benight, A. Bismarck, L.A. Berglund, T. Peijs, Review: current international research into cellulose nanofibres and nanocomposites, J. Mater. Sci. 45 (2010) 1–33, https://doi.org/10.1007/s10853-009-3874-0.

[8] A.J. Uddin, J. Araki, Y. Gotoh, Toward "Strong" sreen nanocomposites: Polyvinyl alcohol reinforced with extremely oriented cellulose whiskers, Biomacromolecules 12 (2011) 617–624, https://doi.org/10.1021/bm101280f.

[9] N. Dogan, T.H. McHugh, Effects of microcrystalline cellulose on functional properties of hydroxy propyl methyl cellulose microcomposite films, J. Food Sci. 72 (2007) E016–E22, https://doi.org/10.1111/j.1750-3841.2006.00237.x.

[10] C.M.O. Müller, J.B. Laurindo, F. Yamashita, Effect of cellulose fibers addition on the mechanical properties and water vapor barrier of starch-based films, Food Hydrocoll. 23 (2009) 1328–1333, https://doi.org/10.1016/j.foodhyd.2008.09.002.

[11] B.L. Peng, N. Dhar, H.L. Liu, K.C. Tam, Chemistry and applications of nanocrystalline cellulose and its derivatives: A nanotechnology perspective, Can. J. Chem. Eng. 89 (2011) 1191–1206, https://doi.org/10.1002/cjce.20554.

[12] A. Balea, E. Fuente, M. Concepcion Monte, N. Merayo, C. Campano, C. Negro, A. Blanco, Industrial application of nanocelluloses in papermaking: A review of challenges, technical solutions, and market perspectives, Molecules 25 (2020) 526, https://doi.org/10.3390/molecules25030526.

[13] D. Roy, M. Semsarilar, J.T. Guthrie, S. Perrier, Cellulose modification by polymer grafting: A review, Chem. Soc. Rev. 38 (2009) 2046–2064, https://doi.org/10.1039/b808639g.

[14] M. Roman, S. Dong, A. Hirani, Y.W. Lee, Cellulose nanocrystals for drug delivery, ACS Symp. Ser. 1017 (2009) 81–91, https://doi.org/10.1021/bk-2009-1017.ch004.

[15] E. Lam, K.B. Male, J.H. Chong, A.C.W. Leung, J.H.T. Luong, Applications of functionalized and nanoparticle-modified nanocrystalline cellulose, Trends Biotechnol. 30 (2012) 283–290, https://doi.org/10.1016/j.tibtech.2012.02.001.

[16] S. Liu, S.A. Qamar, M. Qamar, K. Basharat, M. Bilal, Engineered nanocellulose-based hydrogels for smart drug delivery applications, Int. J. Biol. Macromol. 181 (2021) 275–290, https://doi.org/10.1016/J.IJBIOMAC.2021.03.147.

[17] M. Nogi, S. Iwamoto, A.N. Nakagaito, H. Yano, Optically transparent nanofiber paper, Adv. Mater. 21 (2009) 1595–1598, https://doi.org/10.1002/adma.200803174.

[18] S. Belbekhouche, J. Bras, G. Siqueira, C. Chappey, L. Lebrun, B. Khelifi, S. Marais, A. Dufresne, Water sorption behavior and gas barrier properties of cellulose whiskers and microfibrils films, Carbohydr. Polym. 4 (2011) 1740–1748, https://doi.org/10.1016/J.CARBPOL.2010.10.036.

[19] L.J. Nielsen, S. Eyley, W. Thielemans, J.W. Aylott, Dual fluorescent labelling of cellulose nanocrystals for pH sensing, Chem. Commun. 46 (2010) 8929–8931, https://doi.org/10.1039/c0cc03470c.

[20] I. Kalashnikova, H. Bizot, B. Cathala, I. Capron, Modulation of cellulose nanocrystals amphiphilic properties to stabilize oil/water interface, Biomacromolecules 13 (2012) 267–275, https://doi.org/10.1021/bm201599j.

[21] K.W. Lin, H.Y. Lin, Quality characteristics of chinese-style meatball containing bacterial cellulose (nata), J. Food Sci. 69 (2004) SNQ107–SNQ111. https://doi.org/10.1111/j.1365-2621.2004.tb13378.x.

[22] P.R. Chawla, I.B. Bajaj, S.A. Survase, R.S. Singhal, Microbial cellulose: Fermentative production and applications, Food Technol. Biotechnol. 47 (2009) 107–124.

[23] K.-Y. Lee, G. Buldum, A. Mantalaris, A. Bismarck, More than meets the eye in bacterial cellulose: biosynthesis, bioprocessing, and applications in advanced fiber composites, Macromol. Biosci. 14 (2014) 10–32, https://doi.org/10.1002/mabi.201300298.

[24] H. Yano, J. Sugiyama, A.N. Nakagaito, M. Nogi, T. Matsuura, M. Hikita, K. Handa, Optically transparent composites reinforced with networks of bacterial nanofibers, Adv. Mater. 17 (2005) 153–155, https://doi.org/10.1002/adma.200400597.

[25] D.A. Gregory, L. Tripathi, A.T.R. Fricker, E. Asare, I. Orlando, V. Raghavendran, I. Roy, Bacterial cellulose: A smart biomaterial with diverse applications, Mater. Sci. Eng. R Reports. 145 (2021), 100623, https://doi.org/10.1016/J.MSER.2021.100623.

[26] S.M. Mazhari Mousavi, E. Afra, M. Tajvidi, D.W. Bousfield, M. Dehghani-Firouzabadi, Cellulose nanofiber/carboxymethyl cellulose blends as an efficient coating to improve the structure and barrier properties of paperboard, Cellulose 24 (2017) 3001–3014, https://doi.org/10.1007/s10570-017-1299-5.

[27] D. Klemm, K. Petzold-Welcke, F. Kramer, T. Richter, V. Raddatz, W. Fried, S. Nietzsche, T. Bellmann, D. Fischer, Biotech nanocellulose: A review on progress in product design and today's state of technical and medical applications, Carbohydr. Polym. 254 (2021), https://doi.org/10.1016/J.CARBPOL.2020.117313.

[28] B.G. Rånby III, Fibrous macromolecular systems. Cellulose and muscle. The colloidal properties of cellulose micelles, Discuss. Faraday Soc. 11 (1951) 158–164, https://doi.org/10.1039/DF9511100158.

[29] Y. Habibi, L.A. Lucia, O.J. Rojas, Cellulose nanocrystals: Chemistry, self-assembly, and applications, Chem. Rev. 110 (2010) 3479–3500, https://doi.org/10.1021/cr900339w.

[30] M.A.S. Azizi Samir, F. Alloin, A. Dufresne, Review of recent research into cellulosic whiskers, their properties and their application in nanocomposite field, Biomacromolecules 6 (2005) 612–626, https://doi.org/10.1021/bm0493685.

[31] Z. Karim, S. Afrin, Q. Husain, R. Danish, Necessity of enzymatic hydrolysis for production and functionalization of nanocelluloses, Crit. Rev. Biotechnol. 37 (2017) 355–370, https://doi.org/10.3109/07388551.2016.1163322.

[32] B. Yang, Z. Dai, S.Y. Ding, C.E. Wyman, Enzymatic hydrolysis of cellulosic biomass, Biofuels. 2 (2011) 421–449, https://doi.org/10.4155/bfs.11.116.

[33] A. López-Rubio, J.M. Lagaron, M. Ankerfors, T. Lindström, D. Nordqvist, A. Mattozzi, M.S. Hedenqvist, Enhanced film forming and film properties of amylopectin using micro-fibrillated cellulose, Carbohydr. Polym. 68 (2007) 718–727, https://doi.org/10.1016/j.carbpol.2006.08.008.

[34] A.J. Svagan, M.A.S. Azizi Samir, L.A. Berglund, Biomimetic polysaccharide nanocomposites of high cellulose content and high toughness, Biomacromolecules 8 (2007) 2556–2563, https://doi.org/10.1021/bm0703160.

[35] C. Boisset, C. Fraschini, M. Schülein, B. Henrissat, H. Chanzy, Imaging the enzymatic digestion of bacterial cellulose ribbons reveals the endo character of the cellobiohydrolase Cel6A from Humicola insolens and its mode of synergy with cellobiohydrolase Cel7A, Appl. Environ. Microbiol. 66 (2000) 1444–1452, https://doi.org/10.1128/AEM.66.4.1444-1452.2000.

[36] N.R. Gilkes, E. Jervis, B. Henrissat, B. Tekant, R.C. Miller, R.A.J. Warren, D. G. Kilburn, The adsorption of a bacterial cellulase and its two isolated domains to crystalline cellulose, J. Biol. Chem. 267 (1992) 6743–6749, https://doi.org/10.1016/s0021-9258(19)50488-4.

[37] M. Kostylev, D. Wilson, A distinct model of synergism between a processive endocellulase (TfCel9A) and an exocellulase (TfCel9A) from thermobifida fusca, Appl. Environ. Microbiol. 80 (2014) 339–344, https://doi.org/10.1128/AEM.02706-13.

[38] E.T. Reese, R.G.H. Siu, H.S. Levinson, The biological degradation of soluble cellulose derivatives and its relationship to the mechanism of cellulose hydrolysis, J. Bacteriol. 59 (1950) 485–497, https://doi.org/10.1128/JB.59.4.485-497.1950.

[39] S.J. Horn, G. Vaaje-Kolstad, B. Westereng, V.G.H. Eijsink, Novel enzymes for the degradation of cellulose, Biotechnol. Biofuels. 5 (2012) 45, https://doi.org/10.1186/1754-6834-5-45.

[40] Z. Forsberg, A.K. Mackenzie, M. Sørlie, Å.K. Røhr, R. Helland, A.S. Arvai, G. Vaaje-Kolstad, V.G.H. Eijsink, Structural and functional characterization of a conserved pair of bacterial cellulose-oxidizing lytic polysaccharide monooxygenases, Proc. Natl. Acad. Sci. U. S. A. 111 (2014) 8446–8451, https://doi.org/10.1073/pnas.1402771111.

[41] C. Valls, F.I. Javier Pastor, M. Blanca Roncero, T. Vidal, P. Diaz, J. Martínez, S. V. Valenzuela, Assessing the enzymatic effects of cellulases and LPMO in improving mechanical fibrillation of cotton linters, Biotechnol. Biofuels. 12 (2019) 161, https://doi.org/10.1186/s13068-019-1502-z.

[42] B. Bissaro, A. Várnai, Å.K. Røhr, V.G.H. Eijsink, Oxidoreductases and reactive oxygen species in conversion of lignocellulosic biomass, Microbiol. Mol. Biol. Rev. 82 (2018), https://doi.org/10.1128/mmbr.00029-18.

[43] K.S. Johansen, Lytic polysaccharide monooxygenases: the microbial power tool for lignocellulose degradation, Trends Plant Sci. 21 (2016) 926–936, https://doi.org/10.1016/j.tplants.2016.07.012.

[44] S.V. Valenzuela, G. Ferreres, G. Margalef, F.I.J. Pastor, Fast purification method of functional LPMOs from Streptomyces ambofaciens by affinity adsorption, Carbohydr. Res. 448 (2017) 205–211, https://doi.org/10.1016/j.carres.2017.02.004.

[45] J. Fernández, A.G. Morena, S.V. Valenzuela, F.I.J. Pastor, P. Díaz, J. Martínez, Microbial cellulose from a komagataeibacter intermedius strain isolated from commercial wine vinegar, J. Polym. Environ. 27 (2019) 956–967, https://doi.org/10.1007/s10924-019-01403-4.

[46] T.M. Wood, Preparation of crystalline, amorphous, and dyed cellulase substrates, Methods Enzymol. 160 (1988) 19–25, https://doi.org/10.1016/0076-6879(88)60103-0.

[47] K.R. Birikh, M.W. Heikkila, A. Michine, A. Mialon, T. Grönroos, P. Ihalainen, A. Varho, V. Hämäläinen, A. Suonpää, S.-P. Rantanen, Metgen: Value from Wood - Enzymatic Solutions, in: G. de Gonsalo, P. Dominguez de Maria (Eds.), Biocatalysis: An Industrial Perspective (Catalysis Series), The Royal Society of Chemistry, 2017, pp. 298–322.

[48] G.L. Miller, Use of dinitrosalicylic acid reagent for determination of reducing sugar, Anal. Chem. 31 (1959) 426–428, https://doi.org/10.1021/ac60147a030.

[49] L. Segal, J.J. Creely, A.E. Martin, C.M. Conrad, An empirical method for estimating the degree of crystallinity of native cellulose using the X-ray diffractometer, Text. Res. J. 29 (1959) 786–794, https://doi.org/10.1177/004051755902901003.

[50] P. Falamarzpour, T. Behzad, A. Zamani, Preparation of nanocellulose reinforced chitosan films, cross-linked by adipic acid, Int. J. Mol. Sci. 18 (2017) 396, https://doi.org/10.3390/ijms18020396.

[51] A. Dufresne, Nanocellulose: A new ageless bionanomaterial, Mater. Today. 16 (2013) 220–227, https://doi.org/10.1016/j.mattod.2013.06.004.

[52] S.V. Valenzuela, C. Valls, V. Schink, D. Sánchez, M.B. Roncero, P. Diaz, J. Martínez, F.I.J. Pastor, Differential activity of lytic polysaccharide monooxygenases on celluloses of different crystallinity. Effectiveness in the sustainable production of cellulose nanofibrils, Carbohydr. Polym. 207 (2019) 59–67. https://doi.org/10.1016/j.carbpol.2018.11.076.

[53] O.A. Ogunyewo, A. Randhawa, M. Gupta, V.C. Kaladhar, P.K. Verma, S.S. Yazdani, Synergistic action of a lytic polysaccharide monooxygenase and a cellobiohydrolase from penicillium funiculosum in cellulose saccharification under high-level substrate loading, Appl. Environ. Microbiol. 86 (2020) 1–21, https://doi.org/10.1128/AEM.01769-20.

[54] M.B. Keller, S.F. Badino, N. Røjel, T.H. Sørensen, J. Kari, B. McBrayer, K. Borch, B. M. Blossom, P. Westh, A comparative biochemical investigation of the impeding effect of C1-oxidizing LPMOs on cellobiohydrolases, J. Biol. Chem. 296 (2021), https://doi.org/10.1016/j.jbc.2021.100504.

[55] A. Grząbka-Zasadzińska, A. Skrzypczak, S. Borysiak, The influence of the cation type of ionic liquid on the production of nanocrystalline cellulose and mechanical properties of chitosan-based biocomposites, Cellulose 26 (2019) 4827–4840, https://doi.org/10.1007/s10570-019-02412-1.

[56] C. Buruaga-Ramiro, S.V. Valenzuela, C. Valls, M.B. Roncero, F.I.J. Pastor, P. Díaz, J. Martinez, Development of an antimicrobial bioactive paper made from bacterial cellulose, Int. J. Biol. Macromol. 158 (2020) 587–594, https://doi.org/10.1016/j.ijbiomac.2020.04.234.

[57] E.S. do Nascimento, A.L.S. Pereira, M. de O. Barros, M.K. de A. Barroso, H.L.S. Lima, M. de F. Borges, J.P. de A. Feitosa, H.M.C. de Azeredo, M. de F. Rosa, TEMPO oxidation and high-speed blending as a combined approach to disassemble

bacterial cellulose, Cellulose. 26 (2019) 2291–2302. https://doi.org/10.1007/s10570-018-2208-2.
[58] R.H. Marchessault, F.F. Morehead, M.J. Koch, Some hydrodynamic properties of neutral suspensions of cellulose crystallites as related to size and shape, J. Colloid Sci. 16 (1961) 327–344, https://doi.org/10.1016/0095-8522(61)90033-2.
[59] S. Elazzouzi-Hafraoui, Y. Nishiyama, J.L. Putaux, L. Heux, F. Dubreuil, C. Rochas, The shape and size distribution of crystalline nanoparticles prepared by acid hydrolysis of native cellulose, Biomacromolecules 9 (2008) 57–65, https://doi.org/10.1021/bm700769p.
[60] Y. Van Daele, J.F. Revol, F. Gaill, G. Goffinet, Characterization and supramolecular architecture of the cellulose-protein fibrils in the tunic of the sea peach (Halocynthia papillosa, Ascidiacea, Urochordata), Biol. Cell. 76 (1992) 87–96, https://doi.org/10.1016/0248-4900(92)90198-A.
[61] A.B. Perumal, P.S. Sellamuthu, R.B. Nambiar, E.R. Sadiku, Development of polyvinyl alcohol/chitosan bio-nanocomposite films reinforced with cellulose nanocrystals isolated from rice straw, Appl. Surf. Sci. 449 (2018) 591–602, https://doi.org/10.1016/j.apsusc.2018.01.022.
[62] M. Salari, M. Sowti Khiabani, R. Rezaei Mokarram, B. Ghanbarzadeh, H., Samadi Kafil, Preparation and characterization of cellulose nanocrystals from bacterial cellulose produced in sugar beet molasses and cheese whey media, Int. J. Biol. Macromol. 122 (2019) 280–288, https://doi.org/10.1016/j.ijbiomac.2018.10.136.
[63] J. George, A.S. Bawa, Siddaramaiah, Synthesis and characterization of bacterial cellulose nanocrystals and their PVA nanocomposites, in: Adv. Mater. Res., Trans Tech Publications Ltd, 2010: pp. 383–386. https://doi.org/10.4028/www.scientific.net/AMR.123-125.383.
[64] J. George, Siddaramaiah, High performance edible nanocomposite films containing bacterial cellulose nanocrystals, Carbohydr. Polym. 87 (2012) 2031–2037, https://doi.org/10.1016/j.carbpol.2011.10.019.
[65] D. Klemm, F. Kramer, S. Moritz, T. Lindström, M. Ankerfors, D. Gray, A. Dorris, Nanocelluloses: A new family of nature-based materials, Angew. Chemie Int. Ed. 50 (2011) 5438–5466, https://doi.org/10.1002/anie.201001273.
[66] L. Heux, G. Chauve, C. Bonini, Nonflocculating and chiral-nematic self-ordering of cellulose microcrystals suspensions in nonpolar solvents, Langmuir 16 (2000) 8210–8212, https://doi.org/10.1021/la9913957.
[67] M.M. De Souza Lima, J.T. Wong, M. Paillet, R. Borsali, R. Pecora, Translational and rotational dynamics of rodlike cellulose whiskers, Langmuir 19 (2003) 24–29, https://doi.org/10.1021/la020475z.
[68] A. Dufresne, Nanocellulose, DE GRUYTER (2012), https://doi.org/10.1515/9783110254600.
[69] L. Chen, M. Zou, F.F. Hong, Evaluation of fungal laccase immobilized on natural nanostructured bacterial cellulose, Front. Microbiol. 6 (2015), https://doi.org/10.3389/fmicb.2015.01245.
[70] N.F. Vasconcelos, J.P.A. Feitosa, F.M.P. da Gama, J.P.S. Morais, F.K. Andrade, M. de S.M. de Souza Filho, M. de F. Rosa, Bacterial cellulose nanocrystals produced under different hydrolysis conditions: Properties and morphological features, Carbohydr. Polym. 155 (2017) 425–431. https://doi.org/10.1016/j.carbpol.2016.08.090.
[71] P. Singhsa, R. Narain, H. Manuspiya, Bacterial Cellulose Nanocrystals (BCNC) Preparation and Characterization from Three Bacterial Cellulose Sources and Development of Functionalized BCNCs as Nucleic Acid Delivery Systems, ACS Appl. Nano Mater. 1 (2018) 209–221, https://doi.org/10.1021/acsanm.7b00105.
[72] C.L. Pirich, R.A. de Freitas, M.A. Woehl, G.F. Picheth, D.F.S. Petri, M. R. Sierakowski, Bacterial cellulose nanocrystals: impact of the sulfate content on the interaction with xyloglucan, Cellulose 22 (2015) 1773–1787, https://doi.org/10.1007/s10570-015-0626-y.
[73] Y. Huang, C. Zhu, J. Yang, Y. Nie, C. Chen, D. Sun, Recent advances in bacterial cellulose, Cellulose 21 (2014) 1–30, https://doi.org/10.1007/s10570-013-0088-z.
[74] H. Mirhosseini, C.P. Tan, N.S.A. Hamid, S. Yusof, Effect of Arabic gum, xanthan gum and orange oil contents on ζ-potential, conductivity, stability, size index and pH of orange beverage emulsion, Colloids Surf. A Physicochem. Eng. Asp. 315 (2008) 47–56, https://doi.org/10.1016/J.COLSURFA.2007.07.007.
[75] J.F. Revol, H. Bradford, J. Giasson, R.H. Marchessault, D.G. Gray, Helicoidal self-ordering of cellulose microfibrils in aqueous suspension, Int. J. Biol. Macromol. 14 (1992) 170–172, https://doi.org/10.1016/S0141-8130(05)80008-X.
[76] M. Roman, W.T. Winter, Effect of sulfate groups from sulfuric acid hydrolysis on the thermal degradation behavior of bacterial cellulose, Biomacromolecules 5 (2004) 1671–1677, https://doi.org/10.1021/bm034519+.
[77] M.C.I.M. Amin, A.G. Abadi, H. Katas, Purification, characterization and comparative studies of spray-dried bacterial cellulose microparticles, Carbohydr. Polym. 99 (2014) 180–189, https://doi.org/10.1016/j.carbpol.2013.08.041.
[78] D.M. Panaitescu, A.N. Frone, I. Chiulan, A. Casarica, C.A. Nicolae, M. Ghiurea, R. Trusca, C.M. Damian, Structural and morphological characterization of bacterial cellulose nano-reinforcements prepared by mechanical route, Mater. Des. 110 (2016) 790–801, https://doi.org/10.1016/j.matdes.2016.08.052.
[79] P. Rämänen, P.A. Penttilä, K. Svedström, S.L. Maunu, R. Serimaa, The effect of drying method on the properties and nanoscale structure of cellulose whiskers, Cellulose 19 (2012) 901–912, https://doi.org/10.1007/s10570-012-9695-3.
[80] F.V. Ferreira, A. Dufresne, I.F. Pinheiro, D.H.S. Souza, R.F. Gouveia, L.H.I. Mei, L. M.F. Lona, How do cellulose nanocrystals affect the overall properties of biodegradable polymer nanocomposites: A comprehensive review, Eur. Polym. J. 108 (2018) 274–285, https://doi.org/10.1016/j.eurpolymj.2018.08.045.
[81] Z. Xiang, X. Jin, Q. Liu, Y. Chen, J. Li, F. Lu, The reinforcement mechanism of bacterial cellulose on paper made from woody and non-woody fiber sources, Cellulose 24 (2017) 5147–5156, https://doi.org/10.1007/s10570-017-1468-6.
[82] J. Yuan, T. Wang, X. Huang, W. Wei, Dispersion and beating of bacterial cellulose and their influence on paper properties, BioResources. 11 (2016) 9290–9301. https://doi.org/10.15376/biores.11.4.9290-9301.
[83] C. Aulin, G. Salazar-Alvarez, T. Lindström, High strength, flexible and transparent nanofibrillated cellulose-nanoclay biohybrid films with tunable oxygen and water vapor permeability, Nanoscale. 4 (2012) 6622–6628, https://doi.org/10.1039/c2nr31726e.
[84] C.J. Ridgway, P.A.C. Gane, Constructing NFC-pigment composite surface treatment for enhanced paper stiffness and surface properties, Cellulose 19 (2012) 547–560, https://doi.org/10.1007/s10570-011-9634-8.
[85] S.S. Nair, J. Zhu, Y. Deng, A.J. Ragauskas, High performance green barriers based on nanocellulose, Sustain. Chem. Process. 2 (2014), https://doi.org/10.1186/s40508-014-0023-0.
[86] F. Hoeng, A. Denneulin, J. Bras, Use of nanocellulose in printed electronics: A review, Nanoscale. 8 (2016) 13131–13154, https://doi.org/10.1039/c6nr03054h.
[87] N.L. Garcia de Rodriguez, W. Thielemans, A. Dufresne, Sisal cellulose whiskers reinforced polyvinyl acetate nanocomposites, Cellulose 13 (2006) 261–270, https://doi.org/10.1007/s10570-005-9039-7.
[88] J. Lange, Y. Wyser, Recent innovations in barrier technologies for plastic packaging - a review, Packag. Technol. Sci. 16 (2003) 149–158, https://doi.org/10.1002/pts.621.
[89] M.K.M. Haafiz, A. Hassan, Z. Zakaria, I.M. Inuwa, M.S. Islam, M. Jawaid, Properties of polylactic acid composites reinforced with oil palm biomass microcrystalline cellulose, Carbohydr. Polym. 98 (2013) 139–145, https://doi.org/10.1016/j.carbpol.2013.05.069.
[90] J. Ambrosio-Martín, A. Lopez-Rubio, M.J. Fabra, G. Gorrasi, R. Pantani, J. M. Lagaron, Assessment of ball milling methodology to develop polylactide-bacterial cellulose nanocrystals nanocomposites, J. Appl. Polym. Sci. 132 (2015), https://doi.org/10.1002/app.41605.
[91] M. Martínez-Sanz, M.A. Abdelwahab, A. Lopez-Rubio, J.M. Lagaron, E. Chiellini, T. G. Williams, D.F. Wood, W.J. Orts, S.H. Imam, Incorporation of poly (glycidylmethacrylate) grafted bacterial cellulose nanowhiskers in poly(lactic acid) nanocomposites: Improved barrier and mechanical properties, Eur. Polym. J. 49 (2013) 2062–2072, https://doi.org/10.1016/j.eurpolymj.2013.04.035.
[92] R. Kumar, S. Kumari, B. Rai, R. Das, G. Kumar, Effect of nano-cellulosic fiber on mechanical and barrier properties of polylactic acid (PLA) green nanocomposite film, Mater. Res. Express. 6 (2019), 125108, https://doi.org/10.1088/2053-1591/ab5755.